Microporous and Mesoporous Materials 180 (2013) 235–241

Contents lists available at SciVerse ScienceDirect

Microporous and Mesoporous Materials

journal homepage: www.elsevier.com/locate/micromeso

Role of 3-aminopropyltriethoxysilane in the preparation of mesoporous silica nanoparticles for ibuprofen delivery: Effect on physicochemical properties

N.H.N. Kamarudin [a], A.A. Jalil [a,*], S. Triwahyono [b], N.F.M. Salleh [a], A.H. Karim [b], R.R. Mukti [c], B.H. Hameed [d], A. Ahmad [a]

[a] Institute of Hydrogen Economy, Department of Chemical Engineering, Faculty of Chemical Engineering, Universiti Teknologi Malaysia, 81310 UTM Skudai, Johor, Malaysia
[b] Ibnu Sina Institute for Fundamental Science Studies, Department of Chemistry, Faculty of Science, Universiti Teknologi Malaysia, 81310 UTM Skudai, Johor, Malaysia
[c] Division of Inorganic and Physical Chemistry, Faculty of Mathematics and Natural Science, Institut Teknologi Bandung, Jl Ganesha No. 10, Bandung 40132, Indonesia
[d] School of Chemical Engineering, Engineering Campus, Universiti Sains Malaysia, 14300 Nibong Tebal, Penang, Malaysia

ARTICLE INFO

Article history:
Received 3 March 2013
Received in revised form 31 May 2013
Accepted 28 June 2013
Available online 11 July 2013

Keywords:
Mesoporous silica nanoparticles
Amine
Modification
Ibuprofen
Drug delivery

ABSTRACT

The development of mesoporous silica nanoparticle-based platforms for a controlled drug delivery was studied. Mesoporous silica nanoparticles (MSN) was synthesized and modified with 3-aminopropyltriethoxysilane (APTES) using co-condensation (MSN_{co}) and post-grafting (MSN_{post}) methods. X-ray diffraction (XRD) and transmission electron microscopy (TEM) data confirmed the formation of ordered mesostructured silica nanoparticles. The performance of MSNs was then tested on an ibuprofen immobilization and release. The results revealed that unmodified MSN demonstrated the best immobilization rate and capacity of ibuprofen (98%), MSN_{post} exhibited higher ibuprofen adsorption (78%) as compared to MSN_{co} (71%), suggesting the modification method is not the dominant factor for the adsorption studied. In fact, according to the FT-IR results, the silanol groups density was found to be the contributing factor that affected the adsorption. The *in vitro* drug release was also investigated with simulated biological fluids. In 20 h, MSN_{co} showed the fastest release of ibuprofen (100%), followed by MSN (50%) and MSN_{post} (38%). Both pore size and amine groups influenced the rate of the release process. From the results, MSN and MSN_{post} is suggested to have suitable features for slow drug release which provides constant release over a defined period to avoid repeated administration. While MSN_{co} could be best employed as a fast release system that provides initial burst of drug release to achieve rapid and maximum relief.

1. Introduction

Fortified by the exciting discovery of new kinds of molecular sieves called MS–41 in the early 1990s, exploration on the synthesis of mesoporous silica (MS) materials has received growing attention and advanced rapidly [1–2]. Great endeavors have been made in the tailoring of particle size, pore diameter, morphology, structure, surface properties and functionalization of MS in order to improve their applications in the fields of catalysis, adsorption, and drug delivery [3–6]. As one of the most promising applications in human health care, controlled drug-delivery systems represent an ever-evolving field for biomedical materials science. In recent years, mesoporous silica nanoparticles (MSNs) have been well developed as effective drug storage vehicles in drug delivery systems [7–8] due to their large pore volume (~1 cm^3/g), high surface area (> 1000 m^2/g) [9], ease of functionalization [10], low toxicity and biodegradability [11]. However, one of the main and specific problems of drug delivery system using mesoporous materials is the pore sizes which could not encounter all types of desired drugs which consist of bulky and different features. For this application, the morphology control of MSNs,especially their particle size, dispersivity and pore size are important issues because particles or aggregates with sizes above 300 nm may lead to thrombosis [12] while the pore diameter determines the dimensions of drug molecules which can be loaded in them. In this sense, the synthesis of controllable mesoporous material by an efficient method is a crucial and imperative task.

It is supposed that the drug uptake rate could be modulated by modifying the interaction between the confined molecule and the mesoporous silica medium. This objective could be achieved by functionalization of the pore wall, such as by amine group, carboxylic group, and thiol group. Generally, surface functionalization of mesoporous silica materials via covalent bonding of organic groups can be achieved by two methods: post-grafting synthesis

* Corresponding author. Tel.: +60 7 5535581; fax: +60 7 5536165.
E-mail address: aishah@cheme.utm.my (A.A. Jalil).

1387-1811/$ - see front matter © 2013 Elsevier Inc. All rights reserved.
http://dx.doi.org/10.1016/j.micromeso.2013.06.041

and co-condensation [13]. The resulting functionalized mesoporous materials may help to deliver drugs efficiently and thus, minimize the drugs possible adverse effects [14]. The presence of pores of uniform size lined with silanol groups considers these materials potential interest as host of a variety of guest chemical species, such as amino groups [15].

Amine functionalized mesoporous silica materials have been prepared by several groups for evaluation as a drug delivery medium. Wang et al. reported that amine functionalized samples exhibited higher adsorption capacity for ibuprofen [16]. They also found that the uptake and release of drugs were depended on the type of functional groups in the materials, or the degree of their interaction with drug molecules. Datt et al. reported that the increase in adsorption capacity of aspirin on the amine functionalized MCM-41 materials was attributed to the favorable amine group and aspirin interaction, while co-condensation method was found to engross more drug molecules as compared to post-grafting method [17]. Furthermore, Hoffmann testified that co-condensation method was more accessible and less likely to cause pore blocking relative to comparable samples prepared by the post-synthesis modification [18].

Current efforts in the area of drug delivery also take account of sustained release formulations. Moreover, one of the main targets of current delivery systems in the pharmaceutical industry is to provide a sustained release over time of the active agent in order to maintain its concentration within therapeutic values and below the diligence toxicity threshold [19]. However, a fast release system can also provide an initial burst of drug release. This type of system is used primarily when maximum relief needs to be achieved quickly [20]. On the other hand, a slow release system provides constant rate of release over a defined period of time to avoid repeated administration. Generally, most of the previous studies reported that physical properties changes of the MSN by such amine modification, particularly in the enlargement of pore size has enhanced the adsorption capacity of the drugs [16–18,21]. The release rate is commonly controlled by the interaction between the functional group of the drugs and the introduced amines on the silica surface [22]. The report relating the chemical properties of the MSN on the effective adsorption of drug is still rare. Recently, we found that aside from the role of functionalization, silanol groups were also as a dominating factor that associated to the adsorptivity of the drug. Therefore, to clarify this matter, we modified the MSN with 3-aminopropyltriethoxy-silane via co-condensation and post-grafting methods, and compared their nature with the unmodified MSN. The physicochemical properties of the MSNs were characterized using X-ray powder diffractometry (XRD), transmission electron microscopy (TEM), nitrogen physisorption, field emission scanning electron microscopy (FE-SEM), and fourier transform infrared spectroscopy (FT-IR). The performance of the three MSNs were then examined on the immobilization and release of ibuprofen, which is commonly used as an analgesic and anti-inflammatory drug. The influence of the physicochemical properties of the MSNs towards the model drug delivery system were discussed in detail.

2. Experimental

2.1. Materials

Cetyltrimethylammonium bromide (CTAB), ethylene glycol (EG), tetraethylortho-silicate (TEOS), and 3-aminopropyl triethoxysilane (APTES) were purchased from Merck Sdn Bhd, Malaysia. Ammonium hydroxide (NH_4OH) was obtained from QRec, Malaysia. All the chemicals were used as received without further treatment.

2.2. Synthesis of mesoporous silica nanoparticles (MSN)

MSN were prepared according to the procedure reported in the literature [23–26]. The synthesis procedure was as follows. CTAB, EG, and NH_4OH were dissolved in 700 mL of water with the following molar composition, respectively: 0.0032:0.2:0.2:0.1. After vigorous stirring, TEOS were added to the mixture to give a white micelle solution. The mixture was kept under continuous stirring for 2 h and the sample was collected by centrifugation. The obtained gel was heated at 110 °C for 24 h. To remove the surfactant, the powder was then heated at 550 °C. Complete removal of the surfactant was checked by means of infrared spectroscopy, which did not reveal the presence of any residual organic species.

2.3. Amine modified MSN by the co-synthesis method

APTES was added after the addition of TEOS, while the rest of the procedure remained the same as above. This MSN sample will be hereafter termed MSN_{co}.

2.4. Amine functionalized MSN by the post-grafting method

The post-grafting procedure involved refluxing 1 g of calcined MSN and APTES in toluene at 120 °C for 6 h. The resulting sample was filtered, washed with a 1:1 mixture of dichloromethane and diethyl ether, and dried in an oven at 100 °C. These samples will be referred to as MSN_{post}.

2.5. Materials characterization

The crystallinity of the catalysts was measured with a Bruker Advance D8 X-ray powder diffractometer with Cu Kα (λ = 1.5418 Å) radiation as the diffracted monochromatic beam at 40 kV and 40 mA. TEM was carried out using a JEOL JEM-2100F micro-scope. The samples were ultrasonically dispersed in acetone and deposited on an amorphous, porous carbon grid. Nitrogen physisorption analysis was conducted on a Quantachrome Autosorb-1 at 77 K. The surface morphology and surface elemental analysis of the samples were performed using FESEM-EDX (JEOL JSM-6701F) with an accelerating voltage of 15 kV. FT-IR (Perkin Elmer Spectrum GX FTIR Spectrometer) was performed using the KBr method with a scan range of 400–4000 cm^{-1}. Before the measurement, the sample was evacuated at 573 K for 3 h.

2.6. Ibuprofen loading and release measurements

Powdered mesoporous samples were loaded with ibuprofen by soaking them into an ethanol solution of ibuprofen followed by continuous stirring for 24 h at 310 K. A 1:1 (by weight) ratio of ibuprofen to solid sample was used. In practice, 150 mg of ibuprofen was dissolved in 5 ml of ethanol and 150 mg of dried mesoporous silica were added into this solution. Ibuprofen-loaded samples were recovered by filtration, washed with ethanol and dried for 24 h at 313 K. During the process, aliquots of 2 ml were withdrawn at pre-determined time intervals and centrifuged in a Hettich Zentrifugen Micro 120 before being analyzed by a UV–Vis spectrophotometer (Agilent Technologies) to determine the residual concentration of ibuprofen. Each set of experiments was performed three times. The adsorption band of ibuprofen was taken at a maximum wavelength (λ_{max}) of 264 nm.

The ibuprofen release profile was obtained by adding 0.2 g of the drug-impregnated powders to a 200 mL round-bottom flask containing 100 mL of simulated body fluid (SBF) at 37 °C under continuous stirring. The drug concentration in the release fluid for the different release time was determined using the UV–Vis spectrophotometer. In each case, 3 mL of release fluid were taken

out for analysis of the drug concentration, and then 3 mL of fresh SBF were added to the release system.

3. Results and discussion

3.1. Characterization

The representative XRD data of MSN, MSN_{co} and MSN_{post} in the low 2θ region is shown in Fig. 1. The patterns show three well-resolved Bragg diffraction peaks, at $2\theta = 2.2°$, 3.9° and 4.5° which can be assigned to (100), (110) and (200) reflections of a hexagonal mesoporous structure (P_6mm) typical for MCM-41 type materials [27]. TEM images of the MSNs clearly depict their hexagonal array, with an enhanced structure for the MSN_{co} and a less-ordered structure for MSN_{post} (Fig. 2). According to the XRD result, a strong decrease of the diffraction peak intensity corresponding to the (100) reflection was observed for MSN_{post}, indicating that the long-range ordering of the mesoporous structure decreased significantly with the incorporation of organic groups, but the mesoporous structure was retained after the modification. This is ascribed to the pore filling by APTES groups, which led to the other diffraction peaks (110 and 200) displaying weaker intensities in the MSN_{post} sample [28].

However, a significant increase in intensity was observed for MSN_{co}, demonstrating the enhancement of the ordering of the oxide framework [29]. The introduction of APTES, followed by calcination probably removed the intercalated organic molecules, thereby promoting siloxane cross-linking due to the basal spacing decrease. The APTES groups were thought to be well distributed on the surface of MSN_{co} compared to MSN_{post} because APTES groups were distributed homogeneously on the silica wall during the co-synthesis of the MSN_{co}, leading to a more structured silica skeleton upon calcination. For the MSN_{post}, most organosilane might only concentrated near the opening of the channels and/or on the external surface of the mesopores [18,30]. On the contrary, in a similar study conducted by Datt et al., the introduction of amine group by co-condensation and post-grafting methods to MCM-41 resulted in a decrease in intensity for both modified samples. They reported that this was not only attributed to the pore filling but also partially due to the other factors such as incomplete hydrolysis of the siloxane bridges during the synthesis of mesoporous silica, specifically for the co-condensation method [17].

Fig. 3 shows the nitrogen adsorption–desorption isotherms of MSN, MSN_{co} and MSN_{post} before (Fig. 3A) and after (Fig. 3B) adsorption, whereas Table 1 shows the textural parameters. The MSN demonstrates a typical type IV isotherm with a significant up-step

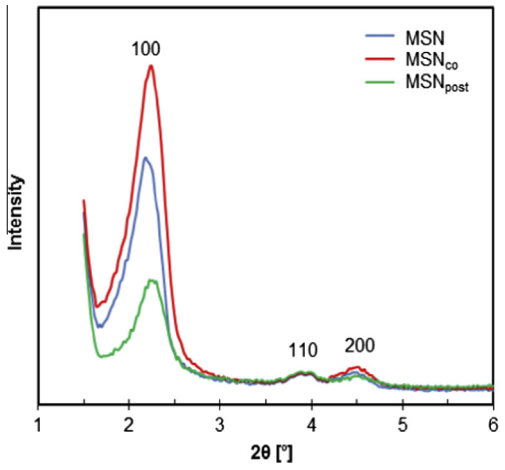

Fig. 1. X-ray diffraction patterns of MSN, MSN_{co}, and MSN_{post}.

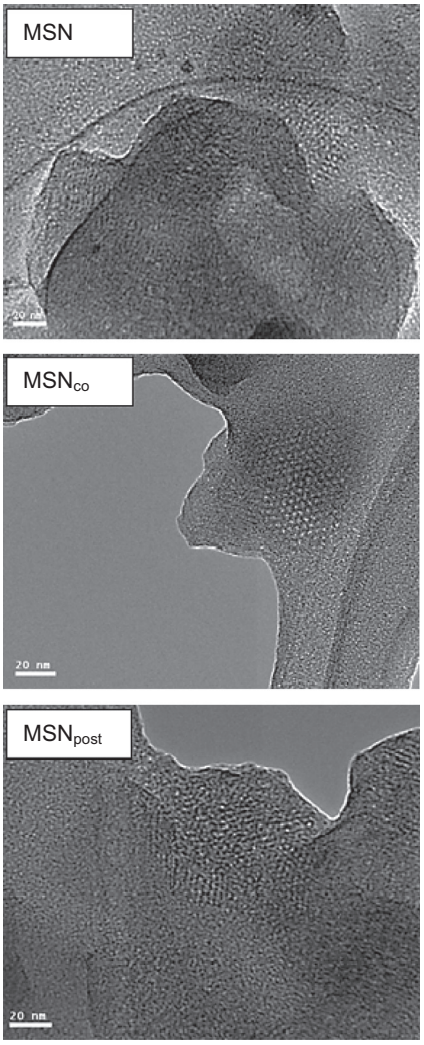

Fig. 2. TEM images of MSN, MSN_{co} and MSN_{post}.

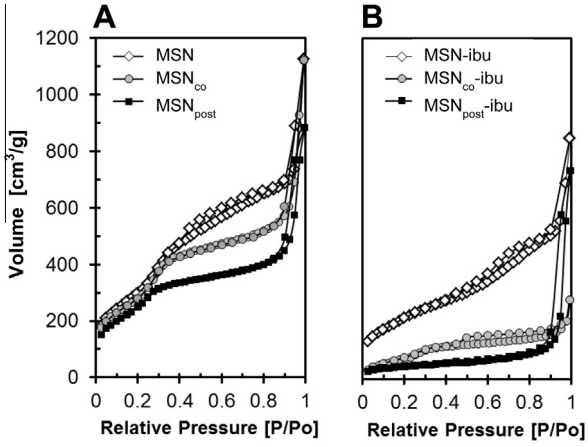

Fig. 3. (A) Nitrogen adsorption–desorption isotherms of MSN, MSN_{co}, and MSN_{post}, (B) Nitrogen adsorption–desorption isotherms of MSN-ibu, MSN_{co}-ibu, and MSN_{post}- ibu.

at a relative pressure of 0.2–0.4, which is associated to the capillary condensation of nitrogen in the channels and also as an indication of narrow pore size distribution [22]. Although the typical adsorption steps clearly remained for MSN_{co}, the solid showed a

Table 1
Textural properties of MSN, MSN_{co} and MSN_{post}.

Sample	Surface area (m^2/g)	Total pore volume (cm^3/g)	Pore size (nm)	d_{100} (nm)
MSN	1107	2.14	3.13	4.05
MSN_{co}	1136	1.73	3.38	3.98
MSN_{post}	992	1.30	3.53	4.09
MSN-IBU	785	1.30	2.98	
MSN_{co}-IBU	955	1.47	3.10	
MSN_{post}-IBU	154	1.10	2.50	

remarkable decrease in nitrogen adsorption when compared to the parent MSN, suggesting that the siloxane cross-linking occurred from the Si that left out from the calcination of APTES groups, which also resulted to the decreased of pore volume. The introduction of APTES by post-modification resulted to the filling of pore voids for MSN_{post}. For all ibuprofen-loaded samples, a significant decrease was also observed in N_2 uptake (Fig. 3B), indicating that ibuprofen molecules were successfully loaded into the pores of the MSNs [31].

Table 1 indicates the distinguishable difference in surface area, total pore volume and pore size of the MSNs. The surface area of MSN was increased when APTES was loaded by co-condensation (MSN_{co}), but reduced by the post-grafting APTES functionalization (MSN_{post}) from 1107 m^2g^{-1} to 1136 m^2g^{-1} and to 992 m^2g^{-1}, respectively. This result is in agreement with the XRD result, confirming the well-ordered structure of MSN_{co} compared to MSN_{post} which had many APTES groups on its surface. The surface area trend is also in parallel with basal spacing of (100) plane. In fact, the reaction was comprehended by the reaction of free silanol groups with ethoxysilanes and resulted in the attachments of aminopropyl functional groups [32]. Accumulation of these functional groups generated a considerable reduction of the surface area and total pore volume. Ghedini et al. expected that the ordered hexagonal array of mesopores has been retained to a certain degree in all modified carriers, but a decrease of the periodic order of the silica supports has occurred upon incorporation of the APTES species [33]. In all cases, ibuprofen loading resulted in a substantial reduction of surface area and total pore volume of the parent samples. It is presumed that ibuprofen molecules in the solvent diffused and drawn into the pores by capillarity, and after solvent removal, the ibuprofen molecules remain trapped in the pore. Accordingly, the pore size was also reduced for all samples, indicating that the pore structures were occupied by ibuprofen molecules. Shen et al. also reported similar observation, in which the ibuprofen loading onto silica supports narrowed the pore size after the pore channels were fully filled [34]. In contrast, the pore size of MSN increased from 3.13 nm to 3.38 nm and 3.53 nm for MSN_{co} and MSN_{post}, respectively, confirming the pore enlargement by the introduction of APTES to the MSN. All samples also showed reduction of the pore width after the loading of ibuprofen, in correlation with the result of surface area and pore volume.

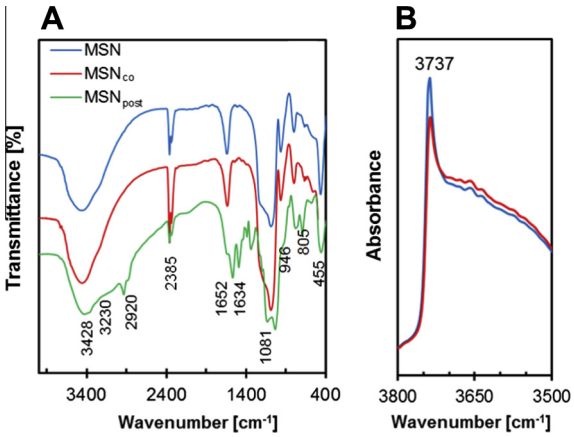

Fig. 5. FT-IR spectra of MSN, MSN_{co} and MSN_{post}.

FESEM images (Fig. 4) demonstrated the formation of spherical MSN materials for all samples, although some were agglomerated. During the sol–gel synthesis, as one of the particles formed, the addition of ethanol while washing the materials reduced the reaction rate which in turn decreased the local surface curvature energy and led to the formation of curved morphologies [35]. MSN_{co} retained the spherical morphology, with a clearer and well-formed spherical shape. The surface void and roughness gradually became lower for the MSN_{post}, suggesting an increase in the density of the nanosphere [36].

FT-IR measurements were performed to identify the structural differences between MSN, MSN_{co} and MSN_{post}. Fig. 5A illustrates the FT-IR spectra of all samples in the range of 400–4000 cm^{-1}. The MSNs exhibited IR peaks at the bands attributed to Si-O-Si bending (455 cm^{-1}), Si-O-Si symmetric stretching (805 cm^{-1}), external Si-OH groups (946 cm^{-1}), Si-O-Si asymmetric stretching (1081 cm^{-1}), water molecules retained by siliceous materials (1652 cm^{-1}), and -OH stretching (3428 cm^{-1}) [37,38]. Band at 2385 cm^{-1} was associated with the asymmetric stretching vibration of gas-phase CO_2 that originates from ambient air absorption in the optical path outside the FT-IR cell [39]. After modification with APTES, the MSN still retained its siliceous structure, displaying no major changes had been occurred in the formation of its framework. The relative intensity of all Si–O vibration modes for MSN_{co} at 455 cm^{-1}, 805 cm^{-1}, 946 cm^{-1}, 1081 cm^{-1} and 1652 cm^{-1} became more intense compared to the parent MSN, particularly at the peak range of 1130–1000 cm^{-1}, suggesting the existence of Si–O–Si interactions at the inner surface of the MSN. The band at 1634 cm^{-1} shown for MSN_{post} could be attributed to the protonated form of amine groups ($-NH_3^+$), which were significant due to the presence of adsorbed water or neighbouring silanol groups [22]. The post-synthetic modification of MSN with amino groups lead to the reaction of free silanol groups with ethoxysilanes and resulted in attachment of aminopropyl functional groups [32].

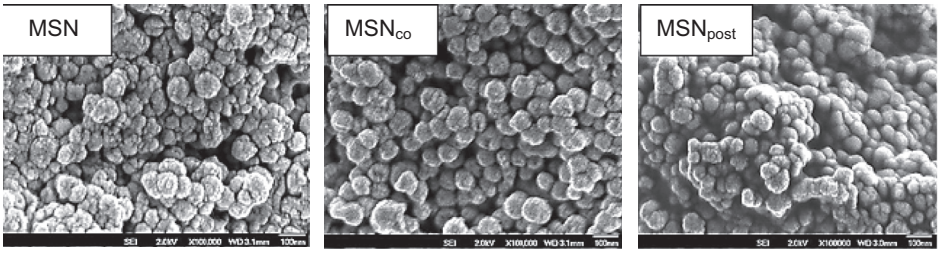

Fig. 4. FESEM images of MSN, MSN_{co} and MSN_{post}.

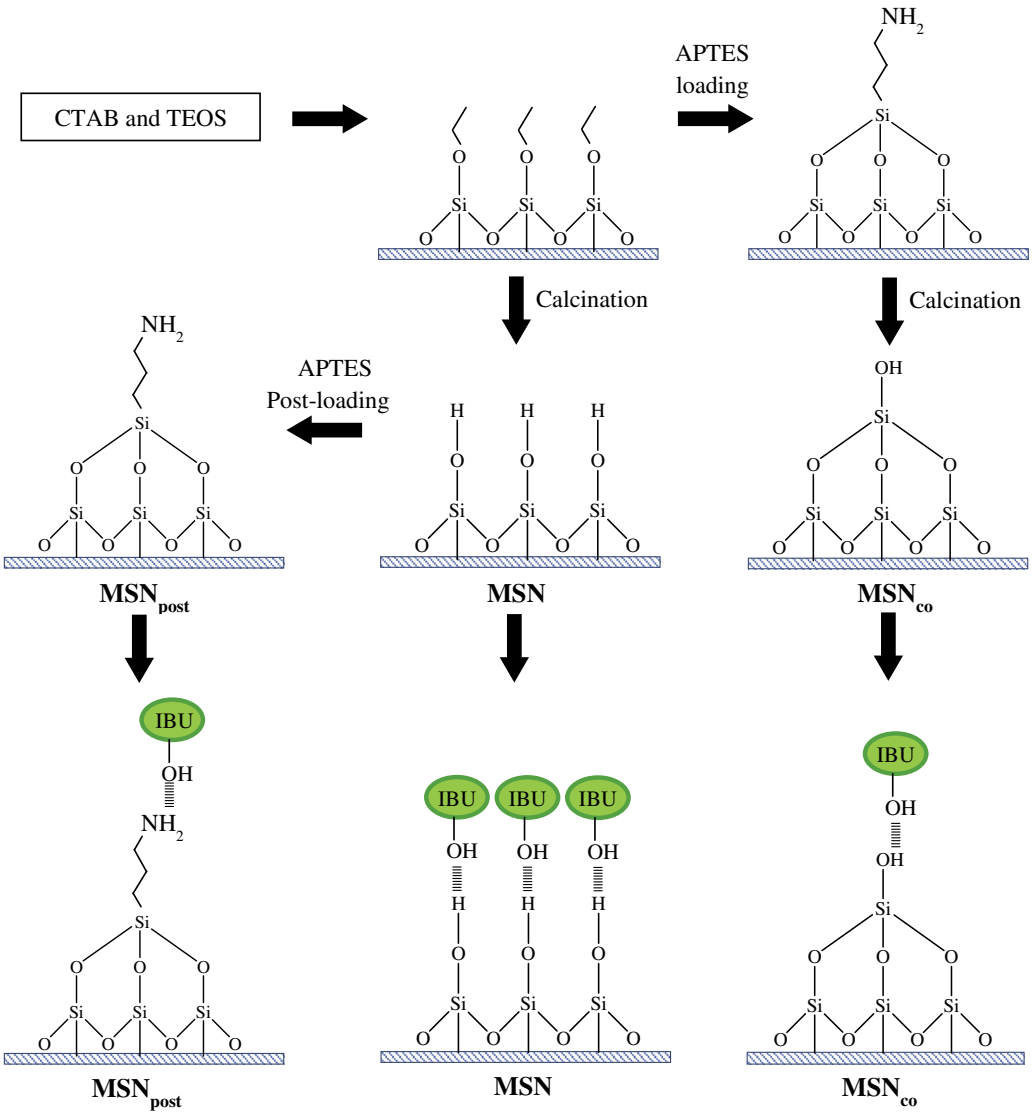

Fig. 6. Speculated mechanism of ibuprofen interaction with silanol group of MSN and MSN_{co}.

FT-IR with evacuation was also conducted to distinguish the silanol group of calcined MSN and MSN_{co} (Fig. 5B). The spectra showed that APTES modification reduced the density of silanol groups at 3737 cm^{-1}. APTES could have promoted the cross-linking of siloxane that resulted from the replacement of an APTES group with the 3-hydroxyl group of Si in the MSN framework, thus decreasing the number of terminal silanol groups significantly (Fig. 6).

3.2. Adsorption of ibuprofen

The performance of MSN, MSN_{co} and MSN_{post} was examined on the adsorption of ibuprofen drug and the result is shown in Fig. 7. The adsorption preceded rapidly when using unmodified MSN, with complete adsorption being achieved after 8 h of reaction. MSN_{co} and MSN_{post} gave slightly lower adsorption percentage, 71% and 78% of maximum adsorption percentage, respectively after 11 h of contact time. In correlation with absolute adsorption amount, the adsorption capacity were 4.85×10^{-4}, 3.44×10^{-4}, and 3.83×10^{-4} mol/g for MSN, MSN_{co} and MSN_{post}, respectively (Table 2). These results indicated that the modification of MSN by APTES hindered the adsorption of ibuprofen. The FTIR results

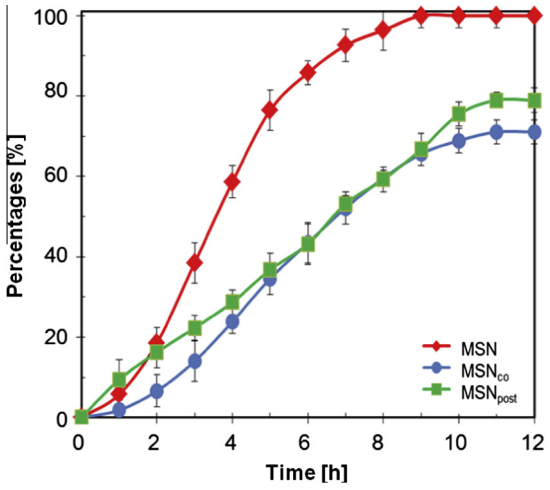

Fig. 7. Adsorption of ibuprofen onto MSN, MSN_{co} and MSN_{post} as a function of contact time.

Table 2
Adsorption and release capacity of ibuprofen for all samples.

Sample	Adsorption capacity ($\times 10^{-4}$ mol/g)	Release capacity (10^{-4} mol/g)
MSN-IBU	4.85	4.53
MSN_{co}-IBU	3.44	3.26
MSN_{post}-IBU	3.83	2.52

suggested that the abundant silanol groups of the parent MSN could be a contributing factor that plays an important role in the hydrogen bond interaction with the carboxyl groups of ibuprofen, which led to the effective adsorption. In this study, the MSN_{post} exhibited higher adsorption for ibuprofen compared to MSN_{co}. This result suggests that the APTES modification order is not the dominant factor for determining the adsorption behavior. The pore size, surface area, and surface functional groups of the mesoporous materials mutually play a significant role in the adsorption [26,40,41].

Based on the above characterization and adsorption results, a mechanism of the modification of MSN with APTES and the interaction of the silanol groups of MSNs with ibuprofen is proposed (Fig. 6). The addition of TEOS to the CTAB mixture produces a silica framework that is then dealkylated to form a parent MSN subsequent to calcination. The post-loading of APTES into this calcined MSN reduces the number of free silanol groups to create new Si–O–Si bonds with aminopropyl functional groups to form MSN_{post}. This speculation was evidenced by FTIR analysis, indicating the increase in intensity for Si–O–Si bonding at band 455 cm^{-1}, 805 cm^{-1}, 946 cm^{-1}, 1081 cm^{-1} and 1652 cm^{-1}, and for protonated amine groups ($-NH_3^+$) at band 1634 cm^{-1}. The decrease in surface area and pore volume may also support this mechanism by confirming the accumulation of APTES groups on the surface of MSN_{post}. Moreover, the introduction of APTES after the addition of TEOS followed by calcination yields the MSN_{co}. This thought is in agreement with the FTIR data which demonstrated a decrease in intensity for the terminal silanol groups at 3737 cm^{-1} for MSN_{co} when compared to parent MSN. The well-ordered silica structure shown by XRD and the increase in surface area and pore size also support this mechanism underlying MSN_{co} formation.

According to the proposed mechanism, the higher density of silanol groups in the parent MSN explains the higher rate of ibuprofen adsorption compared to those of MSN_{co} and MSN_{post} (Fig. 6). The difference in the maximum adsorption percentages of MSN_{post} and MSN_{co} might be due to the strong interaction between the hydroxyl group of ibuprofen and the amine group of APTES compared to that with the silanol group of MSN_{co}. This is may be due to the difference in electronegativity of O and N. The considerable drop in surface area and total pore volume of the ibuprofen-loaded MSN_{post} shown in Table 1 may also supported this fact. This proposed mechanism verifies the important role of silanol groups in the adsorption of ibuprofen. Similar mechanism is also discussed in the literature relating to the possible interaction between the surface silanol groups in the pore walls and the drug [42].

In addition, the variations in pore textural parameters including surface area, pore size, and pore volume have also been reported to affect the adsorption [43]. The pore size of the MSNs shown in Table 1 (>3 nm) is large enough to acommodate ibuprofen, which has a dimension of 1.0 × 5.0 nm^2 [44]. Differences between the inner surfaces of these different sized materials and the packing of ibuprofen inside the channels could also explain the variations in the drug adsorption [21]. The parent MSN showed the largest total pore volume among the others, which may also explain its rapid adsorption rate and the highest adsorption capacity of ibuprofen. A slight difference of the adsorption behavior of MSN_{co} and MSN_{post} may be due to the higher pore volume and pore size of the former and conversely highest accumulation of amine groups on the surfaces of the latter.

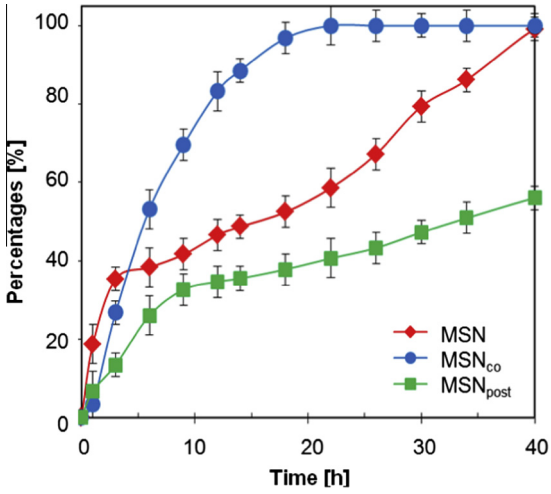

Fig. 8. Release profile of ibuprofen onto MSN, MSN_{co} and MSN_{post} as a function of contact time.

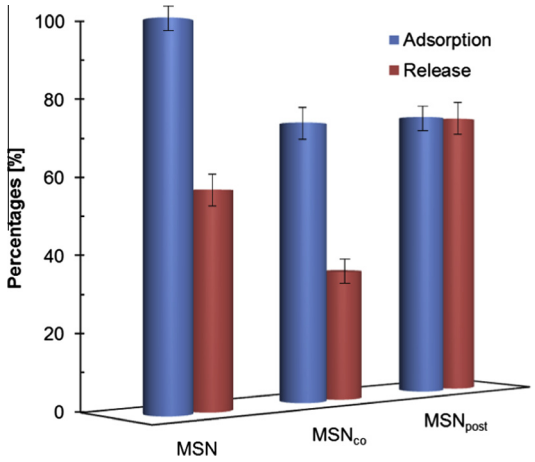

Fig. 9. Immobilization and release profile of ibuprofen onto MSN, MSN_{co} and MSN_{post}.

3.3. Ibuprofen release

To study the performance of MSNs in a drug delivery application, *in vitro* ibuprofen release using a simulated body fluid (SBF) solution was carried out and the profile is shown in Fig. 8. Table 2 displayed the release capacity of 4.53 × 10^{-4} mol/g for MSN, while 3.26 × 10^{-4} mol/g and 2.52 × 10^{-4} mol/g for MSN_{co} and MSN_{post}, respectively. In fact, significant amount of ibuprofen release takes place only when sufficient amount of solvent molecules have diffused through the channels of the mesoporous material for solvation of the drug [45]. The ibuprofen was released faster from MSN_{co}, followed by MSN and MSN_{post}. This may be due to the weaker interaction between the hydroxyl group of ibuprofen and the silanol group of MSN_{co}. Moreover, the parent MSN with a higher number of silanol groups released the ibuprofen gradually until complete release was achieved at 40 h of contact time. The larger pore diameter of MSN_{co} (3.10 nm) in compared to MSN (2.98 nm) and MSN_{post} (2.50 nm) could also played an important role in diffusing the drug molecules out of the pores. MSN_{post} displayed the

slowest release rate of ibuprofen with only 53% of the release percentage in the same contact time when using MSN and MSN_{co}, indicating that the stronger interaction between the the protonated aminopropyl groups and carboxylated anions impeded the process [21].

Fig. 9 summarizes the adsorption and release profiles of ibuprofen for the MSNs. Within 20 h, the adsorbed ibuprofen was released 50% from MSN, 100% from MSN_{co} and 38% from MSN_{post}. From a practical point of view, MSN_{co} could be best employed in fast release system that provides initial burst of drug release for maximum relief that needs to be achieved quickly. Conversely, MSN and MSN_{post} have the most suitable characteristics for slow drug release which provides constant release over a defined period to avoid repeated administration [20,46].

4. Conclusion

MSN was synthesized and modified with APTES using co-condensation (MSN_{co}) and post-grafting (MSN_{post}) methods. The physicochemical properties of the MSNs were characterized by XRD, TEM, N_2 sorption analysis, SEM, and FTIR. Both modification methods displayed different effects on the physicochemical properties of the MSNs. XRD data confirmed the formation of mesostructured silica nanoparticles and also revealed that the MSNs retained their mesoporosity after modification. TEM image showed the hexagonal mesoporous structure of MSNs, which are typical of mesoporous materials. Mechanistic study was conducted to explain the modification path and adsorptivity of the MSN towards ibuprofen delivery. MSN demonstrated the best immobilization rate and capacity of ibuprofen (98%), while, MSN_{post} exhibited higher ibuprofen adsorption (78%) as compared to MSN_{co} (71%), suggesting that the modification method is not the dominant factor for the adsorption studied. In 20 h, MSN_{co} showed the fastest release of ibuprofen (100%), followed by MSN (50%) and MSN_{post} (38%). From FT-IR and surface area analyses, the silanol groups of the MSNs were the contributing factor affecting the rate of adsorption and release of ibuprofen. Furthermore, the pore volume and pore size of the MSNs also slightly influenced the adsorption and release process. This study shows that the MSNs have great potential to be utilized as a host of ibuprofen drug delivery. The MSN and MSN_{post} show suitable features for slow drug release carrier which provides constant release over a defined period to avoid repeated administration. On the other hand, MSN_{co} could be best employed as a fast release system that provides an initial burst of drug release to achieve rapid and maximum relief.

Acknowledgements

The authors are grateful for the financial support by the Research University Grant from Universiti Teknologi Malaysia (Grant no. 02H76), the awards of My PhD Scholarship (Nur Hidayatul Nazirah Kamarudin) from Ministry of Higher Education, Malaysia, and to the Hitachi Scholarship Foundation for their support.

References

[1] C.T. Kresge, M.E. Leonowicz, W.J. Roth, J.C. Vartuli, J.S. Beck, Nature 359 (1992) 710–712.
[2] S. Inagaki, Y. Fukushima, K. Kuroda, J. Chem. Soc., Chem. Commun. (1993) 680–682.
[3] A. Sayari, S. Hamoudi, Chem. Mater. 13 (2001) 3151–3168.
[4] X. Liu, J. Li, L. Zhou, D. Huang, Y. Zhou, Chem. Phys. Lett. 415 (2005) 198–201.
[5] S. Che, Y. Sakamoto, O. Terasaki, T. Tatsumi, Microporous Mesoporous Mater. 85 (2005) 207–218.
[6] Q. Chen, L. Han, C. Gao, S. Che, Microporous Mesoporous Mater. 128 (2010) 203–212.
[7] G.F. Andrade, D.C.F. Soares, R.G. dos Santos, E.M.B. Sousa, Microporous Mesoporous Mater. 168 (2013) 102–110.
[8] J. Gu, S. Su, M. Zhu, Y. Li, W. Zhao, Y. Duan, J. Shi, Microporous Mesoporous Mater. 161 (2012) 160–167.
[9] K. Moeller, J. Kobler, T. Bein, Adv. Funct. Mater. 13 (2007) 605–612.
[10] C.H. Lei, P. Liu, B.W. Chen, Y.M. Mao, H. Engelmann, Y. Shin, J. Jaffar, I. Hellstrom, J. Liu, K.E. Hellstrom, J. Am. Chem. Soc. 132 (2010) 6906–6907.
[11] F. Sevimli, A. Yılmaz, Microporous Mesoporous Mater. 158 (2012) 281–291.
[12] C.B. Barbe, J. Bartlett, L. Kong, K. Finnie, H.Q. Lin, M. Larkin, S. Calleja, A. Bush, G. Calleja, Adv. Mater. 16 (2004) 1959–1966.
[13] M.S. Kim, J.B. Jeon, J.Y. Chang, Microporous Mesoporous Mater. 172 (2013) 118–124.
[14] D. Zhao, J. Feng, Q. Huo, N. Melosh, G.H. Fredrickson, B.F. Chmelka, G.D. Stucky, Science 279 (1998) 549–552.
[15] K. Moller, T. Bein, Chem. Mater. 10 (1998) 2950–2963.
[16] G. Wang, A.N. Otuonye, E.A. Blair, K. Denton, Z. Tao, T. Asefa, J. Sol. State Chem. 182 (2009) 1649–1660.
[17] A. Datt, I. El-Maazawi, S.C. Larsen, J. Phys. Chem. C 116 (2012) 18358–18366.
[18] F. Hoffmann, M. Cornelius, J. Morell, M. Froba, Angew. Chem. Int. Ed. 45 (2006) 3216–3251.
[19] W. Zhao, H. Zhang, S. Chang, J. Gu, Y. Li, L. Li, J. Shi, RSC Adv. 2 (2012) 5105–5107.
[20] C.M. Lopes, J.M.S. Lobo, J.F. Pinto, P.C. Costa, AAPS Pharm. Sci. Tech. 8 (2007) 3–10.
[21] B. Munoz, A. Ramila, J. Perez-Pariente, I. Diaz, M. Vallet-Regi, Chem. Mater. 15 (2003) 500–503.
[22] A. Szegedi, M. Popova, I. Goshev, J. Mihaly, J. Sol. State Chem. 184 (2011) 1201–1207.
[23] R.R. Mukti, H. Hirahara, A. Sugawara, A. Shimojima, T. Okubo, Langmuir 26 (4) (2010) 2731–2735.
[24] A.H. Karim, A.A. Jalil, S. Triwahyono, S.M. Sidik, N.H.N. Kamarudin, R. Jusoh, N.W.C. Jusoh, B.H. Hameed, J. Coll. Interf. Sci. 386 (2012) 307–314.
[25] A.A. Jalil, N. Kurono, M. Tokuda, Synlett 12 (2001) 1944–1946.
[26] A.A. Jalil, N. Kurono, M. Tokuda, Synthesis 18 (2002) 2681–2686.
[27] T. Heikkila, H.A. Santos, N. Kumar, D.Y. Murzin, J. Salonen, T. Laaksonen, L. Peltonen, J. Hirvonen, V.-P. Lehto, Eur. J. Pharm. Biopharm. 74 (3) (2010) 483–494.
[28] Q. Tang, Y. Xu, D. Wu, Y. Sun, J. Wang, J. Xu, F. Deng, J. Control. Rel. 114 (2006) 41–46.
[29] W. Xiaozhong, D. Tao, X. Yongzhuang, L. Yuping, J. Nat. Gas Chem. 9 (2000) 40–49.
[30] T. Yokoi, H. Yoshitake, T. Tatsumi, J. Mater. Chem. 14 (6) (2004) 951–957.
[31] A.S. Al-Kady, M. Gaber, M.M. Hussein, E.-Z.M. Ebeid, Eur. J. Pharm. Biopharm. 77 (1) (2011) 66–74.
[32] Z. Luan, J.A. Fournier, J.B. Wooten, D.E. Miser, Microporous Mesoporous Mater. 83 (2005) 150–158.
[33] E. Ghedini, M. Signoretto, F. Pinna, D. Guarascio, G. Cerrato, Stud. Surf. Sci. Catal. 174 (2008) 429–432.
[34] S.-C. Shen, W.K. Ng, L. Chia, J. Hu, R.B.H. Tan, Int. J. Pharm. 410 (2011) 188–195.
[35] A. Katiyar, S. Yadav, P.G. Smirniotis, N.G. Pinto, J. Chromatogr. A 1122 (2006) 13–20.
[36] X. Du, J. He, J. Coll. Interf. Sci. 345 (2) (2010) 269–277.
[37] A.M. Klonkowski, T. Widernik, B. Grobelna, W.K. Jozwiak, H. Proga, E. Szubiakiewicz, J. Sol-Gel. Sci. Technol. 20 (2) (2001) 161–180.
[38] L.P. Singh, S.K. Agarwal, S.K. Bhattacharyya, U. Sharma, S. Ahalawat, Nanomater. Nanotech. 1 (2011) 44–51.
[39] B.S. Caglayan, A.E. Aksoylu, J. Hazard. Mater. 252–253 (2013) 19–28.
[40] A. Szegedi, M. Popova, I. Goshev, S. Klébert, J. Mihály, J. Solid State Chem. 194 (2012) 257–263.
[41] D.H. Hwang, D. Lee, H. Lee, D. Choe, S.H. Lee, K. Lee, Korean J. Chem. Eng. 27 (4) (2010) 1087–1092.
[42] J. Andersson, J. Rosenholm, M. Linden, in: N. Ashammakhi (Ed.), Topics in Multifunctional Biomaterials and Devices e-book, vol. 1, 2008, pp. 1–19.
[43] Q. Tang, Y. Chen, J. Chen, J. Li, Y. Xu, D. Wu, Y. Sun, J. Solid State Chem. 183 (1) (2010). 76-73.
[44] V. Nakayanan, Materials Research 11 (4) (2008) 443–446.
[45] S. Kapoor, R. Hegde, A.J. Bhattacharyya, J. Control. Rel. 140 (2009) 34–39.
[46] A. Fini, V. Bergamante, G.C. Ceschel, C. Ronchi, C.A.F. de Moraes, Eur. J. Pharm. Biopharm. 69 (1) (2008) 335–341.